

## Metastable crystalline and amorphous carbon phases obtained from fullerite C<sub>60</sub> by high-pressure–high-temperature treatment

V. V. Brazhkin, A. G. Lyapin, S. V. Popova, R. N. Voloshin, and Yu. V. Antonov  
*Institute for High Pressure Physics, Russian Academy of Sciences, Troitsk, Moscow region, 142092, Russia*

S. G. Lyapin\*  
*Clarendon Laboratory, Physics Department, University of Oxford, Parks Road, Oxford OX1 3PU, England*

Yu. A. Kluev and A. M. Naletov  
*Russian Scientific-Research Institute of Diamonds, 119110, Moscow, Russia*

N. N. Mel'nik  
*Lebedev Physics Institute, Russian Academy of Sciences, 117924, Moscow, Russia*

(Received 21 January 1997; revised manuscript received 14 April 1997)

A number of metastable ordered and disordered carbon phases have been prepared from fullerite C<sub>60</sub> by heating to different temperatures at 12.5 GPa and subsequent quenching to ambient conditions. We studied the structure, Raman spectra, and hardness of the phases obtained. The increase of synthesis temperature up to 500 °C leads to a gradual three-dimensional polymerization and subsequent formation of a disordered network with a high share of  $sp^3$  sites. Further increase of the synthesis temperature leads to the formation of graphitelike clusters and then crystallization of graphite and diamond at  $T \sim 900$  °C. The structure of the polymer phases was identified as fcc, the lattice parameter value decreasing down to  $\sim 11.6$  Å with increase of synthesis temperature. A model of three-dimensional polymerization explaining the observed structural modification is proposed. The model allows one to calculate the share of covalently bonded molecules and describes the change of mechanical properties of polymeric phases in terms of rigidity percolation. Experimental results obtained for strongly polymerized states which favor a polymerization mechanism, other than [2+2] cycloaddition are discussed. [S0163-1829(97)07141-5]

### I. INTRODUCTION

Phase transformations in C<sub>60</sub> fullerite have been actively studied in a wide pressure range for the last six years. A majority of recent papers concerning temperature-induced transformations in fullerite under pressure dealt with pressures  $P \leq 9$  GPa. One- and two-dimensional (1D or 2D) polymerization has been observed at pressures  $P \leq 8$  GPa,<sup>1-5</sup> and several polymorphic forms of solid C<sub>60</sub> have been synthesized. Polymerization of fullerite is associated with the formation of covalent  $sp^3$  bonds between molecules via the [2+2] cycloaddition mechanism.<sup>6-10</sup> The polymer phases may be reverted to pristine C<sub>60</sub> by heating at ambient pressure,<sup>1,3</sup> and hence may be treated as metastable phases of the molecular fullerite crystal. Three-dimensional (3D) polymerization,<sup>5,11,12</sup> occurring at  $P > 8$  GPa, is not well studied now, and the mechanism of such transformations is practically unclear.

Under high-temperature and high-pressure conditions, fullerite C<sub>60</sub> was found to transform into amorphous carbon phases of different nature,<sup>11-19</sup> microcrystalline graphite,<sup>11,18,20</sup> and cubic diamond,<sup>15,16,18,21</sup> both in static and shock compression experiments. All these transformations are accompanied by irreversible collapse of C<sub>60</sub> molecules.

It is well known that atoms in solid carbon phases may exist in  $sp^2$  or  $sp^3$  states. A variation of the average atomic valency during the transformation of fullerite to polymerized and disordered phases is of great interest from both fundamental and applied points of view. One can indicate the three

main classes of metastable carbon phases prepared from C<sub>60</sub> under pressure: (i) polymerized phases with covalently bonded C<sub>60</sub> molecules, (ii) amorphous states with collapsed molecules and varied fraction of  $sp^2$  or  $sp^3$  sites, (iii) disordered phases with diamond or graphite microcrystals. In this paper we investigate carbon phases from all the three groups, which have been prepared upon heating at  $P = 12.5$  GPa with subsequent quenching to ambient conditions. One should emphasize that the pressure-temperature region under consideration ( $290 < T \leq 1200$  K and  $P = 12.5$  GPa) is still a gray area on the “phase diagram” of fullerite. Particular interest is directed to understanding the structural mechanism of transformation from C<sub>60</sub> crystal to amorphous phase through 3D polymers, before graphitization of the sample. We investigated x-ray diffraction, Raman spectra, and hardness of 3D fullerite polymers and amorphous phases.

In Sec. III we present the main experimental results. In Sec. IV we propose the model of 3D polymerization, supported by a set of experimental data. Some aspects of order-disorder and  $sp^2$ - $sp^3$  transformations in fullerite C<sub>60</sub> under pressure-temperature treatment, including experimental evidence for a polymerization mechanism other than the [2+2] cycloaddition, will be discussed in Sec. V.

### II. EXPERIMENT

The samples were synthesized from fullerite powder produced at Russian Scientific Center “Kurchatov Institute,” with the C<sub>60</sub> content not less than 99.9% and 50-100 μm

crystalline grains. The powder of  $C_{60}$  microcrystals was formed into 2-mm high and 2-mm diameter cylinders. A new version of the “toroid” chamber<sup>22</sup> was used for high-pressure–high-temperature generation (up to 13 GPa in the temperature range 300–2000 K) in a large volume (up to 30 mm<sup>3</sup>). The samples were placed into Pd or Pt cells and heated by passing electric current through the outer graphite container.

The density of samples was determined by the Archimed method. The structure of samples was investigated by conventional x-ray diffraction (Cu  $K\alpha$ ). Raman measurements were performed at 300 K using Jobin-Yvon T64000 triple grating spectrometer with a nitrogen-cooled multichannel CCD detector. The typical bandpass was less than 2 cm<sup>-1</sup>. The 514.5 nm line of Ar<sup>+</sup> laser was used for excitation, and the beam was focused to a spot less than 10  $\mu$ m in diameter. All Raman spectra presented here were independent of the excitation intensity, which was typically within the range 0.1–15 mW. The radiation power of the laser was chosen to prevent the photopolymerization effects.<sup>6</sup> The Raman spectra were taken in the true backscattering configuration with incident and scattered polarizations orthogonal to each other. The hardness was investigated by means of indenting the diamond Vickers pyramids under loads 1.96 and 5.5 N.

### III. STRUCTURE AND RAMAN SPECTRA

The samples were subject to different temperatures under pressure 12.5 GPa, and their structure was investigated after quenching the samples to the ambient conditions. The x-ray patterns of the samples prepared at relatively low temperatures  $T_{\text{syn}} \leq 450$  °C revealed distinct crystalline reflections (Fig. 1). The structure of all crystalline phases prepared was identified as fcc. The lattice parameter  $a$  was found to decrease with increasing synthesis temperature  $T_{\text{syn}}$  (Table I), simultaneously with increase in the degree of disorder. The calculated crystallographic densities are in good agreement with the experimental data (Table I).

The calculated and measured intensities of (111), (200), and (220) reflections are compared in Fig. 2. The calculations were based upon the geometry of the experiment, atomic scattering factors, the number of reflecting atomic planes, and the molecular factor  $F_{\text{mol}}$  in the uniform sphere approximation, i.e.,  $F_{\text{mol}} \propto \sin(QR)/QR$  (see, for example, Ref. 23), where  $Q$  is the scattering wave vector and  $R$  is the radius of the fullerene molecule [ $R \approx 3.5$  Å (Ref. 23)]. The theoretical and experimental intensities are in satisfactory agreement for the phases with the lattice parameter  $a \geq 12.3$  Å. The behavior of the intensities observed suggests that the  $C_{60}$  molecules can be regarded as structure-forming units in the case of crystalline phases with  $a \geq 12.3$  Å. The samples heated to higher temperatures  $T_{\text{syn}} \approx 450$  °C (9 and 10) revealed essential distortion and possibly destruction of the spherelike  $C_{60}$  molecules (Fig. 2).

A decrease of the lattice parameter in these phases indicates the appearance of stronger interaction between the molecules due to formation of covalent bonds,<sup>6–9</sup> i.e., polymerization. Considering the molecular radius to be  $R \approx 3.5$  Å, the average intermolecular distance for 3D-polymerized samples (5–8) must be  $\approx 1.6$  Å, that is close enough to the length of covalent bonds in fullerene polymers.<sup>3,7–9,24</sup> Both

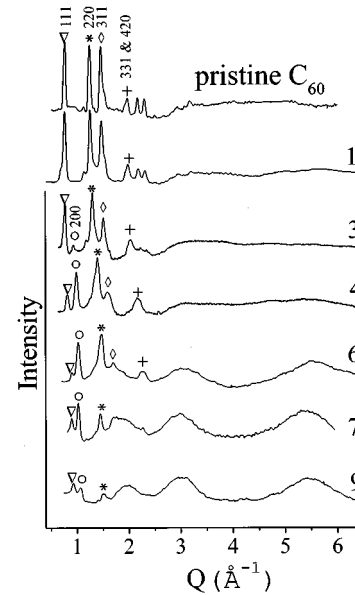


FIG. 1. X-ray diffraction patterns (with subtracted middle lines) for the polymerized crystalline phases of fullerite  $C_{60}$  prepared at 12.5 GPa. Numeration of the curves is the same as in Table I. The similar fcc reflections are marked by identical symbols.

calculations<sup>7–9,24</sup> and experiments<sup>3</sup> show that in the cases of polymerized dimer, chain, as well as 1D and 2D fullerene polymers the intermolecular distance varies in the range 9–9.2 Å which corresponds to the period  $a \approx 12.7$  Å for the fcc lattice. So it would be reasonable to consider the crystalline samples 5–8 as the 3D polymers of fullerite. Significant distortion and/or destruction of the convex  $C_{60}$  molecules in strongly polymerized samples 9 and 10 ( $a < 12$  Å) are evidently due to weak compressibility of the covalent bonds that restrict further mutual uniform approach of the molecules to each other. The broad amorphous peaks at  $Q \approx 3$  and  $5.5$  Å<sup>-1</sup> visible in the x-ray-diffraction patterns of the polymerized phases correspond to amorphous carbon with  $sp^3$  sites,<sup>25–27</sup> and may be associated with the appearance of the covalent  $sp^3$  bonds between  $C_{60}$  molecules.

The heating to 500 °C leads to a complete disorder in the structure of fullerite (see Fig. 3). The x-ray diffraction pattern of the corresponding sample (11) revealed broad lines around 3 and  $5.5$  Å<sup>-1</sup> associated with  $sp^3$  amorphous carbon.<sup>25–27</sup> The  $sp^2$ -rich forms of amorphous carbon display broad lines around 2 and  $3$  Å<sup>-1</sup>, having approximately the same intensity.<sup>26,28,29</sup> This indicates a considerable share of  $sp^3$  sites in the amorphous sample 11 and agrees well with the density 3.15 g/cm<sup>3</sup> (Table I) typical for amorphous films containing  $\sim 80$ –90% of  $sp^3$  sites.<sup>30</sup> The line at  $Q \approx 1.4$  Å<sup>-1</sup> shows a maintaining of certain ordering, or correlation, which may be connected to the initial molecular structure, because the corresponding interlayer distance  $d \sim 4.5$  Å is approximately equal to half the intermolecular distance in strongly polymerized phases.

Further heating under pressure evokes narrowing of the line around  $3$  Å<sup>-1</sup> and the appearance of the two new peaks at  $\sim 2$  and  $\sim 4$  Å<sup>-1</sup>, clearly identified as the (002) and (004) reflections from parallel-packed hexagonal planes of graphite (Fig. 3). Upon strong heating  $\sim 900$  °C the location of the (002) reflection corresponds to the tabulated value for crys-

TABLE I. Parameter of fcc lattice  $a$ , calculated  $\rho_{\text{calc}}$ , and experimentally measured  $\rho_{\text{exp}}$  densities, and hardness  $H_V$  for polymerized fullerite samples and disordered phases obtained from  $C_{60}$  under pressure  $P = 12.5$  GPa at various synthesis temperatures  $T_{\text{syn}}$ .

Sample	$T_{\text{syn}}$ (°C)	$a$ (Å)	$\rho_{\text{calc}}$ (g/cm <sup>3</sup> ) <sup>a</sup>	$\rho_{\text{exp}}$ (g/cm <sup>3</sup> )	$H_V$ (GPa)
1	20	14.04±0.01	1.73	1.7	
2	100	14.03±0.08	1.73	1.75	0.15±0.05
3	150	13.5±0.1	1.95	1.9	4.2±0.6
4	200	12.95±0.1	2.20	2.3	33.6±2.2
5	300	12.3±0.2	2.57	2.5	25.7±0.8
6	300	12.25±0.1	2.60		36±7
7	400	12.27±0.03	2.59	2.8	26.4±0.7
8	450	12.23±0.03	2.62		44.0±1.2
9	450	11.95±0.05	2.80	3.0	52±6
10	450	11.62±0.06	3.05	3.1	65±5
11	500	Disordered		3.15	76.4±0.6
12	600	Disordered		3.0	75.4±1.1
13	700	Disordered		3.2	69±6
14	900	Disordered		3.0	87±10

Uncertainty ±10% ±0.15

<sup>a</sup>Crystallographic density  $\rho_{\text{calc}}$  was calculated using experimental lattice parameter  $a$ .

talline graphite, whereas at lower synthesis temperatures the hexagonal layers should be somewhat squeezed. The size of graphitic clusters along the  $z$  axis can be evaluated from the linewidth of the (002) and (004) reflections. The calculation gives  $\sim 25$  Å for samples with  $T_{\text{syn}} \sim 600$ – $700$  °C, that is equivalent to  $\sim 8$  graphite layers, and  $\sim 50$  Å for higher synthesis temperatures. With the temperature increase crystallization of  $sp^3$  sites into diamond microcrystals occurs since the (111) diamond line becomes narrow, and the (220) and (311) diamond reflections come into view though weak and diffused (sample 14).

The Raman spectra for the pristine  $C_{60}$  and some of the polymerized phases are presented in Fig. 4. Our spectra for the pristine  $C_{60}$  and the polarization relationships for the line intensities are in good agreement with the literature data.<sup>31–33</sup> The Raman spectra of the slightly polymerized  $C_{60}$  phase (sample 3) revealed clearly the narrow lines corresponding to the fullerene modes. New lines 300 and 527  $\text{cm}^{-1}$  are visible

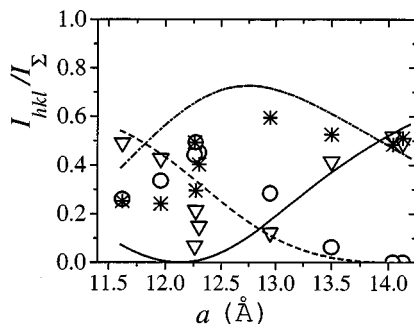


FIG. 2. Calculated dependences and experimental data (symbols) for intensities of the (111) (solid line and triangles), (200) (dashed line and circles), and (220) (dashed and dotted line and stars) reflections vs lattice parameter.

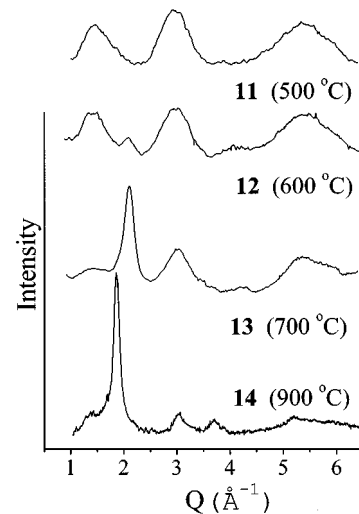


FIG. 3. X-ray-diffraction patterns for disordered carbon phases prepared from fullerite  $C_{60}$  at 12.5 GPa.

in this spectrum. These lines are similar to those that become Raman active in the pristine  $C_{60}$  under pressure  $P > 0.4$  GPa (Ref. 33) and in photopolymerized  $C_{60}$ .<sup>6</sup> Apart from the narrow lines, the broadbands (1100–1600  $\text{cm}^{-1}$  and 250–600  $\text{cm}^{-1}$ ) are seen in the Raman spectrum of sample 3 (Fig. 4). The samples with higher polymerization degree (4 and 8) have broadbands (200–800 and 1200–1700  $\text{cm}^{-1}$ ) in their Raman spectra, which are usual for the amorphous phases, although x-ray-diffraction patterns of these samples definitely reveal their crystalline nature (Fig. 1).

The Raman spectrum of a completely disordered phase differs from those of strongly polymerized phases and looks very much like the spectrum of amorphous carbon with a high degree of  $sp^3$  bonding.<sup>30</sup> It is well known<sup>34</sup> that the Raman features of  $sp^3$  bonding are difficult to observe because of their much lower cross section ( $\sim 1/50$ ) than that for  $sp^2$  bonding. So, the spectra obtained reflect the activity of  $sp^2$  sites. The increase of the synthesis temperature

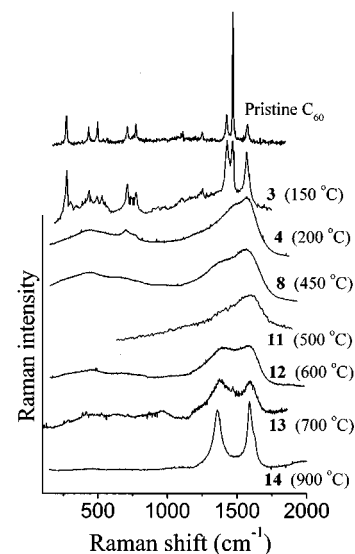


FIG. 4. Raman spectra, measured in the perpendicular geometry, for carbon phases prepared from fullerite  $C_{60}$ .

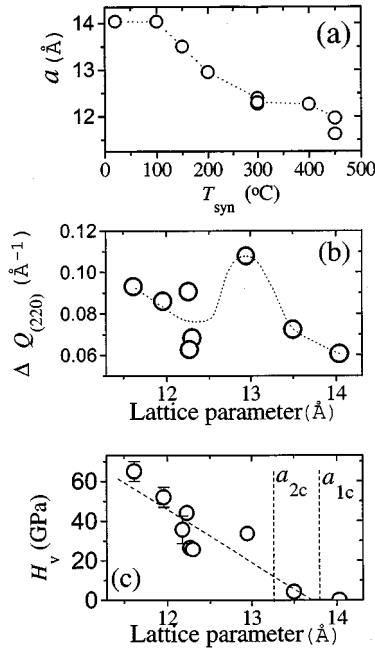


FIG. 5. Some characteristics of the fcc 3D-polymerized phases: the lattice parameter vs synthesis temperature (a) and the FWHM for the (220) reflection (b) and hardness (c) vs lattice parameter. The dotted lines are guidance for eyes. The vertical dashed lines correspond to different rigidity percolation thresholds.

(samples 12–14) leads to the appearance of a distinct doublet structure in the Raman spectra with the maxima of the lines being located within the intervals 1360–1420 and 1580–1600  $\text{cm}^{-1}$ . Taking into account the results of x-ray-diffraction study, these two lines can be identified as the graphite Raman-active  $G$  line and the interlayer “disordered”  $D$  line observable in microcrystalline graphite.<sup>35–37</sup> The change of spectra with increase of synthesis temperature is qualitatively analogous to that obtained during the crystallite formation in amorphous carbon films.<sup>37</sup> The broadening of Raman lines is connected with the bond-angle disorder in hexagonal layers. We believe one reason for such disorder to be the interplanar  $sp^3$  linkage, that explains squeezing of the hexagonal layers observed from structural data.

#### IV. MODEL FOR THREE-DIMENSIONAL POLYMERIZATION OF FULLERITE $C_{60}$

##### A. Polymerization of fcc phases

The dependence of the lattice parameter on the synthesis temperature has a quasicontinuous character for fcc 3D-polymerized fullerite phases. [Fig. 5(a)] The fcc phases with relatively large lattice parameters have been obtained previously.<sup>1,12</sup> So it is natural to suppose the possible existence of the fcc polymers with any lattice parameter within the range from 14.17 Å (pristine  $C_{60}$ ) to  $\sim 11.6$  Å (strongly polymerized phases obtained in the current study). This means the average intermolecular distance can vary from 3 to 1.4 Å.

The calculations for different polymer configurations of  $C_{60}$  molecules give the intermolecular bond length about  $\sim 1.6$  Å,<sup>7–9</sup> comparable with that in diamond 1.54 Å. Theoretical analysis also shows that the formation of two covalent

intermolecular bonds ( $[2+2]$  cycloaddition mechanism) is much more favorable energetically than the alternative polymerization mechanisms.<sup>7</sup>

The main idea of the model proposed is the assumption that a pair of nearest molecules can in fact be found in two states being connected by the covalent or van der Waals forces, while the observable period of the fcc lattice is a continuous function of the share of covalently bonded (polymerized) molecular pairs and is obtained by means of the averaging procedure throughout the lattice with varying degree of disorder in the types and lengths of bonds. This suggests the existence of uniform and random (or quasirandom) distribution of polymerized pairs over the lattice.

The van der Waals lattice of pristine  $C_{60}$  and completely 3D-polymerized phase with a certain lattice parameter  $a_p$  would be the extremities for a set of 3D polymeric phases. The lower limit of the lattice parameter range, in which the spherical molecular factor approximation holds (Fig. 2), would be an appropriate approximation for  $a_p$ , i.e.,  $a_p \sim 12.3$  Å. This parameter corresponds to an intermolecular distance of 8.7 Å which is very close to the sum of the  $C_{60}$  molecule diameter ( $\approx 7$  Å) and the length of covalent  $sp^3$  bonds in carbon ( $\sim 1.54$ – $1.6$  Å), and we will use the estimation  $a_p \approx 12.3$  Å. In our approach the distortion of  $C_{60}$  molecules in the fcc phases with  $a_p < 12$  Å is caused by the strong repulsion between covalently bonded atoms of adjacent molecules. So, probably polymerization mechanisms other than the  $[2+2]$  cycloaddition, for example, the formation of four bonds between molecules,<sup>7</sup> become prevalent.

The model proposed treats partly polymerized fullerite as a substitution solid solution, with different types of bonds instead of different atoms. Analogous to the Vegard’s law for solid solutions, the lattice parameter of a partially polymerized phase can be linearly approximated as a function of the share of polymerized molecular pairs  $n_p$

$$a = a_0 + (a_p - a_0)n_p, \quad (1)$$

which, as in the case of solutions, is connected with the relaxation of intermolecular stresses.

By analogy with substitution solid solutions, the static dispersion of atomic positions connected with the disorder of the bond types must exist in a fcc crystal with two characteristic lengths of the bonds. The highest fluctuations of atomic locations would be present for  $n_p \sim 0.5$ , that means equal share of both van der Waals and covalent bonds. These fluctuations must influence the width of crystalline reflections on the x-ray-diffraction pattern. Figure 5(b) shows the full width at half maximum (FWHM)  $\Delta Q$  for the (220) peak vs lattice parameter. This reflection was chosen due to its moderately large intensity in the x-ray patterns for all fcc phases. The largest width was obtained for the phase with  $a \approx 13$  Å, intermediate between the 3D-polymerized and depolymerized states. The analogous behavior was revealed by the (111) and (200) reflections.

##### B. Rigidity percolation in fcc polymers of the fullerite $C_{60}$

One more advantage of the model considered is the prediction of the mechanical properties of 3D fcc phases. Covalent bonds are much more rigid than van der Waals bonds. The bulk modulus of the pristine fullerite is  $\sim 18$  GPa,<sup>23</sup>

which is an order of magnitude less than that of covalent diamond. If the lattice parameter of a fcc polymer is close to that of the pristine fullerite, the share of polymerized pairs is small according to Eq. (1), so just a few clusters would be covalently bonded. Such a situation apparently has been obtained for the photopolymerization process.<sup>6</sup> The phases with  $a \rightarrow a_0$  would be as soft as the pristine fullerite itself and cannot be treated rigorously as 3D-polymerized phases. For  $a \rightarrow a_p$ , we, in fact, deal with a rigid covalent network which is corroborated by the experimental measurements of hardness (See Table I).

The elastic rigidity percolation defined by the degree of covalency between molecules seems to be an appropriate description of a transition between the two extremities if we consider the contribution of van der Waals forces to be negligible. A 3D network of covalently bonded atoms becomes rigid when the average coordination number reaches or exceeds the value of  $Z_{1c} = 2.4$ .<sup>38</sup> The average coordination number of covalently bonded pairs of  $C_{60}$  molecules  $Z_p$  would be defined by their share  $n_p$  as  $Z_p = n_p Z$ , where  $Z = 12$  is the coordination number of a fcc lattice. Considering the threshold intermolecular coordination number for the appearance of hardness and elasticity in a system of covalently bonded  $C_{60}$  molecules to be  $Z_{1c} = 2.4$ , we obtain the threshold concentration  $n_{1c} = 0.2$  and the corresponding lattice period  $a_{1c} \approx 13.8 \text{ \AA}$  [see Eq. (1)].

Covalent bonds possess the angular rigidity diminishing the number of freedom degree in the system. In our case the upper limit for the threshold rigidity value may be obtained if we consider the bonds without the angular rigidity. Then, the rigidity percolation appears when three bonds per molecule correspond to three translational degrees of freedom for each molecule (rotations of rigidly connected molecules may be excluded). The critical coordination number is  $Z_{2c} = 6$ .<sup>39</sup> For the upper limit of rigidity we obtain the critical concentration of covalently bonded pairs of molecules  $n_{2c} = 0.5$  and the lattice period  $a_{2c} \approx 13.2 \text{ \AA}$ .

Figure 5(c) shows the dependence of the hardness for the fcc phases of fullerite vs the lattice parameter, which completely supports the picture described above. The hardness continuously increases with the average coordination number for molecules similar to the increase of elastic constant in the models mentioned.<sup>38,39</sup> Linear interpolation with the least-squares fitting gives the threshold parameter close to the first one,  $a_{1c} \approx 13.7 \text{ \AA}$ . The growth of hardness for the phases with  $a < a_p$ , when polymerization is considered complete in the framework of this model, is probably connected to the further increase of the number of covalent bonds between molecules due to their deformation and partial destruction.

## V. DISCUSSION

The sequence of carbon phases synthesized under pressure corresponds to the successive structural transformations taking place on heating at 12.5 GPa. The structural and Raman data show that the increase of the synthesis temperature evokes both disordering of the location of  $C_{60}$  molecules and their destruction with the formation of the amorphous  $sp^2$ - $sp^3$  network.

The first evidence for disordering may be seen from the Raman spectra (Fig. 4). At the intermediate stage of 3D po-

lymerization the disorder in the system may be connected to the presence of different types of intermolecular bonds. However, the reason for the appearance of the amorphous carbonlike Raman spectra seems to be somewhat different. The icosahedral point-symmetry group of an individual  $C_{60}$  molecule ( $I_h$ ) and the point-symmetry group of fcc lattice ( $O_h$ ) have the point-symmetry group of tetrahedron  $T_h$  as the common subgroups. This gives a possibility for construction of the 3D fcc polymer with the  $T_h$  symmetry. Nevertheless, the random character of formation of covalent bonds between the molecules in 3D polymers causes an orientational disorder. The appearance of covalent  $sp^3$  intermolecular bonds (almost tetrahedrally oriented) should enforce local tensions and slight distortions in  $C_{60}$  molecules. As a result, the Raman spectra of strongly polymerized phases look completely ‘‘amorphous.’’ Unlike 3D polymers, both 1D- and 2D-polymerized phases reveal clearly crystalline Raman spectra.<sup>1,4,5</sup>

The Raman spectrum of some 3D polymer sample (e.g., 3) displays both ‘‘crystalline’’ and ‘‘amorphous’’ features. Apparently, the reason for this is the different degree of intermolecular covalent connectivity for different molecules. About 30% of molecular pairs in sample 3 ( $a = 13.5 \text{ \AA}$ ) must be covalently bonded, according to Eq. (1). This value exceeds substantially both the rigidity threshold in the system ( $n_{1c} = 0.2$ ) and the percolation threshold for the formation of three-dimensional infinite cluster ( $n_c Z \approx 1.43$  or  $n_c \approx 0.12$ ) in the fcc lattice.<sup>40</sup>

To analyze the mechanism of order-disorder transition the knowledge of the  $sp^3$  sites share is of great importance. A natural assumption arises that the initial stage of 3D polymerization is due to the  $[2+2]$  cycloaddition mechanism, which is much more favorable energetically.<sup>7</sup> This means that four  $sp^3$  atoms correspond to each covalently bonded pair of  $C_{60}$  molecules. The share of  $sp^3$  atoms in 3D polymer can be defined by the share of bonded molecular pairs  $n_p$  from the equation

$$N_{sp^3} = \frac{2n_p Z}{60}, \quad (2)$$

where  $Z = 12$  is the fcc-lattice coordination number. A maximum value of  $N_{sp^3} = 0.4$  is reached at  $a = a_p$  for the completely 3D-polymerized fullerite.

Using Eqs. (1) and (2) one can obtain the dependence of  $N_{sp^3}$  vs the crystallographic density  $\rho$  (Fig. 6), if we choose the value of  $a_p$  from the realistic domain 12.2–12.6  $\text{\AA}$ . One should note that the density values for the completely polymerized phases with  $a \sim a_p$  are rather close to those for the corresponding amorphous carbon films<sup>30</sup> with  $\sim 40\%$  of fourfold atomic sites (Fig. 6), thus supporting the consideration of the 3D-polymerized phases as  $sp^2$ - $sp^3$  networks. The partially polymerized fullerene fcc phases ( $a > a_p$ ) are less dense than the corresponding amorphous samples. Further decrease of the lattice parameter ( $a < a_p$ ) and density increase should apparently be accompanied by a further fast increase of the share of  $sp^3$  sites, according to the data for amorphous films. In the framework of the views on the polymerization of  $C_{60}$  molecules the mechanism of this increase can be connected to the formation of four covalent bonds between molecules instead of two bonds (see Ref. 7).

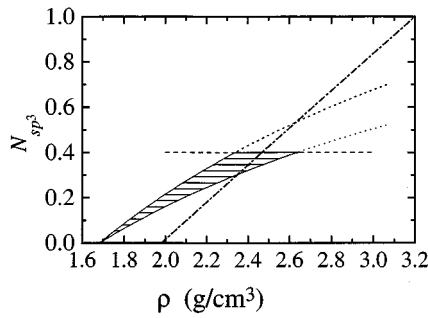


FIG. 6. Concentration of  $sp^3$  atomic sites vs density dependences for the amorphous carbon films from Ref. 30 (dashed and dotted line) and 3D-polymerized phases of fullerite  $C_{60}$  (shaded area). The last is calculated using Eqs. (1) and (2), where  $2.2 \leq a_p \leq 2.6 \text{ \AA}$ . The horizontal dashed line correspond to the maximum concentration of  $sp^3$  sites, when 3D polymerization occurs via the  $[2+2]$  cycloaddition mechanism.

This is in good agreement with the strong deformation of initially spherical pristine  $C_{60}$  units in the fcc phases with  $a < a_p$  (Fig. 2). For the new mechanism of polymerization the maximum share of  $sp^3$  sites in a fcc polymer may be equal to  $4Z/60 = 0.8$ . It is interesting to note that the atomic network of the collapsed  $C_{60}$  sample simulated under pressure by the tight-binding molecular-dynamics calculation<sup>41</sup> gave the value of share of  $sp^3$  sites to be 79%. The  $N_{sp^3}(\rho)$  dependence for the fullerite compressed in this simulation consists of intervals of slow and fast increase of  $N_{sp^3}$ , which is in good accordance with the analysis shown above. The mechanical characteristics and densities of both the strong polymerized phase and “diamondlike” amorphous carbon (sample 11) are rather adequate to such a high share of four-fold atoms.

Other evidence of the growing disorder in the system is the appearance of the amorphous peak around  $3 \text{ \AA}^{-1}$  in the structure factor (Fig. 1). It can be assumed that the intensity of this peak is defined by scattering from  $sp^3$  sites (including four nearest-neighbors forming a tetrahedron for each such site) and is proportional to the share of  $sp^3$  sites. The relative intensity of this peak vs lattice parameter is presented in Fig. 7. The intensity change is relatively small in the interval  $a_p < a < a_0$ , where  $a_p \approx 12.3 \text{ \AA}$ , whereas a much more rapid increase of the intensity takes place for  $a < a_p$  or  $\rho > 2.5 \text{ g/cm}^3$ . The experimental pattern agrees well with the above analysis based on Fig. 6.

## VI. CONCLUSION

A set of metastable carbon phases obtained by heating  $C_{60}$  fullerite under the pressure 12.5 GPa were investigated in this paper by x-ray diffraction, Raman spectroscopy, and hardness measurements. High-pressure–high-temperature

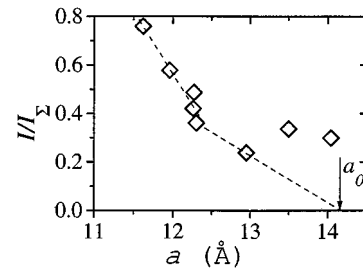


FIG. 7. Relative intensity of the wide x-ray-diffraction peak around  $3 \text{ \AA}^{-1}$  as a function of density. The summarized intensity  $I_{\Sigma}$  was obtained by summation of areas under all peaks in the range  $Q \leq 3.5 \text{ \AA}^{-1}$ . The dashed lines are guides for the eyes.

( $\sim 900 \text{ }^\circ\text{C}$ ) treatment of  $C_{60}$  evokes a transformation to a microcrystalline graphite-diamond mixture. The transformation occurs through a number of intermediate 3D-polymerized crystalline and disordered phases.

The structure of 3D-polymerized modifications was identified as fcc. The analysis of the intensity of x-ray crystalline peaks shows that the pristine  $C_{60}$  units retain their spherical symmetry in the range of lattice parameters 12.3–14.17  $\text{ \AA}$ , while the distortion of  $C_{60}$  molecules occurs at lower lattice parameter values. A model of 3D polymerization is proposed for the first stage of polymerization ( $a \geq 12.3 \text{ \AA}$ ), which relates the fcc lattice parameter to the share of covalently bonded molecular pairs. The model explains a set of structural anomalies and the changes of mechanical properties of 3D-polymerized phases in terms of rigidity percolation. The approach given is strictly supported by experimental data. The Raman spectra of strongly polymerized phases look analogous to those of amorphous carbon, that may be explained by the incompatibility of point-symmetry groups for single  $C_{60}$  molecule and fcc lattice. Careful analysis of experimental data allowed us to suppose the importance of a polymerization mechanism other than  $[2+2]$  cycloaddition at the second stage of 3D polymerization ( $a \leq 12.3 \text{ \AA}$ ), preceding the formation of the amorphous network with a high degree of  $sp^3$  bonding. Further heating leads to an increase of heterogeneity in disordered phases and induces the appearance of graphitelike  $sp^2$  clusters.

## ACKNOWLEDGMENTS

The work was financially supported by the Russian Fund for Fundamental Research (Grant Nos. 95-02-03677 and 96-02-17328a). The authors are grateful to Professor S. M. Stishov and Yu. A. Osipyanyan for useful discussions, to N. V. Kalyaeva, N. I. Epishina, and T. I. Bulygina for assistance with measurements of mechanical properties, to Dr. M. Grimsditch for preliminary Raman measurements of some samples, and to Dr. R. A. Sadykov for assistance in x-ray experiments.

\*On leave from Institute for High Pressure Physics, Russian Academy of Sciences, Troitsk, Moscow region, 142092, Russia; electronic address: s.lyapin@physics.ox.ac.uk

<sup>1</sup>Y. Iwasa, T. Arima, R. M. Fleming, T. Siegrist, O. Zhou, R. C. Haddon, L. J. Rothberg, K. B. Lyons, H. L. Carter, Jr., A. F. Hebard, R. Tycko, G. Dabbagh, J. J. Krajewski, G. A. Thomas,

and T. Yagi, *Science* **264**, 1570 (1994).

<sup>2</sup>I. O. Bashkin, V. I. Rashupkin, A. F. Gurov, A. P. Moravsky, O. G. Rybchenko, N. P. Kobelev, Y. M. Soifer, and E. G. Ponyatovsky, *J. Phys. Condens. Matter* **6**, 7491 (1994).

<sup>3</sup>M. N  n  z-Regueiro, L. Marques, J-L. Hodeau, O. B  thoux, and M. Perroux, *Phys. Rev. Lett.* **74**, 278 (1995).

- <sup>4</sup>C. S. Sundar, P. Ch. Sahu, V. S. Sastry, G. V. N. Rao, V. Sridharan, M. Premila, A. Bharathi, Y. Hariharan, T. S. Radhakrishnan, D. V. S. Muthu, and A. K. Sood, *Phys. Rev. B* **53**, 8180 (1996).
- <sup>5</sup>U. D. Venkateswaran, D. Sanzi, J. Krishnappa, L. Marques, J.-L. Hodeau, M. Núñez-Regueiro, A. M. Rao, and P. C. Eklund, *Phys. Status Solidi B* **198**, 545 (1996).
- <sup>6</sup>A. M. Rao, P. Zhou, K.-A. Wang, G. T. Hager, J. M. Holden, Y. Wang, W.-T. Lee, X.-X. Bi, P. C. Eklund, D. S. Cornett, M. A. Duncan, and I. J. Amster, *Science* **259**, 955 (1993).
- <sup>7</sup>G. B. Adams, J. B. Page, O. F. Sankey, and M. O’Keeffe, *Phys. Rev. B* **50**, 17 471 (1994).
- <sup>8</sup>M. R. Pederson and A. A. Quong, *Phys. Rev. Lett.* **74**, 2319 (1995).
- <sup>9</sup>D. Porezag, M. R. Pederson, T. Frauenheim, and T. Kohler, *Phys. Rev. B* **52**, 14 963 (1995).
- <sup>10</sup>C. Goze, F. Rachdi, L. Hajji, M. Núñez-Regueiro, L. Marques, J.-L. Hodeau, and M. Mehring, *Phys. Rev. B* **54**, R3676 (1996).
- <sup>11</sup>V. V. Brazhkin, A. G. Lyapin, Yu. V. Antonov, S. V. Popova, Yu. A. Klyuev, A. M. Naletov, and N. N. Mel’nik, *Pis’ma Zh. Eksp. Teor. Fiz.* **62**, 328 1995 [*JETP Lett.* **62**, 350 (1995)].
- <sup>12</sup>V. D. Blank, S. G. Buga, N. R. Serebryanaya, V. N. Denisov, G. A. Dubitsky, A. N. Ivlev, B. N. Mavrin, and M. Yu. Popov, *Phys. Lett. A* **205**, 208 (1995); V. D. Blank, S. G. Buga, N. R. Serebryanaya, G. A. Dubitsky, S. N. Sulyanov, M. Yu. Popov, V. N. Denisov, A. N. Ivlev, and B. N. Mavrin, *ibid.* **220**, 149 (1996).
- <sup>13</sup>J. Haines and J. M. Leger, *Solid State Commun.* **90**, 361 (1994).
- <sup>14</sup>D. W. Snoke, Y. S. Raptis, and K. Syassen, *Phys. Rev. B* **45**, 14 419 (1992).
- <sup>15</sup>C. S. Yoo, W. J. Nellis, M. L. Satler, and R. G. Musket, *Appl. Phys. Lett.* **61**, 273 (1992).
- <sup>16</sup>M. Núñez-Regueiro, L. Abello, G. Lucazeau, and J. L. Hodeau, *Phys. Rev. B* **46**, 9903 (1992).
- <sup>17</sup>S. D. Kosowsky, C. H. Hsu, N. H. Chen, F. Moshary, P. S. Pershan, and I. F. Silvera, *Phys. Rev. B* **48**, 8474 (1993).
- <sup>18</sup>J. L. Hodeau, J. M. Tonnerre, B. Bouchet-Fabre, M. Núñez-Regueiro, J. J. Capponi, and M. Perroux, *Phys. Rev. B* **50**, 10 311 (1994).
- <sup>19</sup>H. Hirai, K. Kondo, N. Yoshizawa, and M. Shiraishi, *Appl. Phys. Lett.* **64**, 1797 (1994); H. Hirai, Y. Tabira, K. Kondo, T. Oikawa, and N. Ishizawa, *Phys. Rev. B* **52**, 6162 (1995).
- <sup>20</sup>C. S. Yoo and W. J. Nellis, *Science* **254**, 1489 (1991).
- <sup>21</sup>M. Núñez-Regueiro, P. Monceau, and J. L. Hodeau, *Nature (London)* **355**, 237 (1992).
- <sup>22</sup>L. G. Khvostantsev, L. F. Vereshchagin, and A. P. Novikov, *High Temp.-High Press.* **9**, 637 (1977).
- <sup>23</sup>S. J. Duclos, K. Brister, R. C. Haddon, A. R. Kortan, and F. A. Thiei, *Nature (London)* **351**, 380 (1991).
- <sup>24</sup>C. H. Xu and G. E. Scuseria, *Phys. Rev. Lett.* **74**, 274 (1995).
- <sup>25</sup>P. H. Gaskell, A. Saeed, P. Chieux, and D. R. McKenzie, *Phys. Rev. Lett.* **67**, 1286 (1991).
- <sup>26</sup>P. C. Kelires, *Phys. Rev. B* **47**, 1829 (1993).
- <sup>27</sup>B. R. Djordjević, M. F. Thorpe, and F. Wooten, *Phys. Rev. B* **52**, 5685 (1995).
- <sup>28</sup>F. Li and J. S. Lannin, *Phys. Rev. Lett.* **65**, 1905 (1990).
- <sup>29</sup>C. Z. Wang, K. H. Ho, and C. T. Chan, *Phys. Rev. Lett.* **70**, 611 (1993).
- <sup>30</sup>M. Weiler, S. Sattel, T. Giessen, K. Jung, H. Ehrhardt, V. S. Veerasamy, and J. Robertson, *Phys. Rev. B* **53**, 1594 (1996).
- <sup>31</sup>D. S. Bethune, G. Meijer, W. C. Tang, H. J. Rosen, W. G. Golden, H. Seki, C. A. Brown, and M. S. de Vries, *Chem. Phys. Lett.* **179**, 181 (1991).
- <sup>32</sup>P. H. M. van Loosdrecht, P. J. M. van Bentum, M. A. Verheijen, and G. Meijer, *Chem. Phys. Lett.* **198**, 587 (1992).
- <sup>33</sup>K. P. Meletov, D. Christofilos, S. Ves, G. A. Kourouklis, *Phys. Rev. B* **52**, 10 090 (1995).
- <sup>34</sup>R. E. Shroder, R. J. Nemanich, and J. T. Glass, *Phys. Rev. B* **41**, 3738 (1990).
- <sup>35</sup>F. Tuinstra and J. L. Koenig, *J. Chem. Phys.* **53**, 1126 (1970).
- <sup>36</sup>R. J. Nemanich and S. A. Solin, *Phys. Rev. B* **20**, 392 (1979).
- <sup>37</sup>R. O. Dillon, J. Woollam, and V. Katkanant, *Phys. Rev. B* **29**, 3482 (1984).
- <sup>38</sup>H. He and M. F. Thorpe, *Phys. Rev. Lett.* **54**, 2107 (1985).
- <sup>39</sup>S. Feng, M. F. Thorpe, and E. Garboczi, *Phys. Rev. B* **31**, 276 (1985).
- <sup>40</sup>R. Zallen, *The Physics of Amorphous Solids* (Wiley, New York, 1983), p. 170.
- <sup>41</sup>B. L. Zhang, C. Z. Wang, K. M. Ho, and C. T. Chan, *Europhys. Lett.* **28**, 219 (1994).